EAST EUROPEAN JOURNAL OF PHYSICS. 1. 484-489 (2026)
DOI:10.26565/2312-4334-2026-1-55 ISSN 2312-4334

# IMPLEMENTATION OF HARMONIC MAPPING TO A CLOAK PHENOMENON

**Najma Abdul Rehman[1], Muhammad Raza[1], Oleg Rybin[2]*, Sergey Shulga[2]**
[1]*Department of Mathematics, COMSATS University Islamabad, Sahiwal Campus, Sahiwal, Pakistan*
[2]*School of Radio Physics, Biomedical Electronics & Computer Systems,*
*V.N. Karazin Kharkiv National University, Kharkiv, Ukraine*
**Corresponding Author email: oleg.rybin@karazin.ua*
Received November 11, 2025; revised February 7, 2026; accepted February 24, 2026

In this work, a novel physical transformation-based approach has been employed to realize the cloak effect. The transformation mapping is derived for the first time by minimizing the energy functional subject to specified geometric constraints on the scatterer's boundaries. This variational problem has been solved using a physics-informed neural network to solve the boundary-value problem for the Laplace equation. Numerical analysis and graphical visualization of the obtained results clearly demonstrate weak scattering and distortion, as well as negligible perturbation to exterior fields. Furthermore, we show that the proposed mapping achieves considerably improved performance compared with conventional transformation-based cloaking methods, which can be used to mask compact radiating devices, particularly patch antennas.
**Keywords:** *Harmonic maps; Physics-informed neural network; Cloaking; Laplace equation; Energy functional minimization*
**PACS**: 41.20.Cv; 02.70.-c

## 1. INTRODUCTION

Research on harmonic maps originated from the study of harmonic functions and the Dirichlet principle. Indeed, Joseph Sampson [1], James Eells, and L. Lemaire [2] formally introduced harmonic maps as a generalization of harmonic functions to maps between Riemannian manifolds, defining them as the critical points of an associated energy functional [2]. Harmonic maps have a strong mathematical foundation because they preserve both the shape and the continuity of the underlying objects. Due to its analytical and geometric properties, the theory of harmonic maps has a wide range of applications in physics, including quantum physics, fluid dynamics, gravitation, electrostatics, image processing, and learning-based studies [3-7].

Transformation optics is a fundamental approach for designing invisibility cloaks by using coordinate transformations to control physical fields across a wide range of subjects [8-10]. In electromagnetic and Optics, Transformation optics (TO) aims to map the behaviour of light around an object/scatterer from virtual space to a transformed physical space, thereby controlling the bending and propagation of light to achieve cloaking invisibility [11-13]. In fact, the main idea behind cloaking is that an appropriate coordinate transformation maps a virtual space into a physical space, and the material parameters required for field guidance are derived from the transformation's Jacobian. Initially, the method was applied to the transformation of Maxwell's equations; later, this framework was extended to other governing equations under various coordinate transformations [10, 14-18]. This, in turn, shows that developing mapping approaches is a direct path toward establishing TO as a multidisciplinary research subject.

In this study, we model the cloak phenomenon using harmonic maps rather than a conventional coordinate transformation. We show that harmonic maps, as critical points of an energy functional, naturally yield smooth, regularized cloaking transformations. Furthermore, the elements of the tensor of material parameters derived from this transformation are generally bounded, which leads to a low distortion field manipulation. By employing harmonic maps, undesirable scattering can be considerably reduced. Moreover, the harmonic maps are combined with transformation optics and a physics-informed neural network (PINN) based approach to achieve the desired invisibility effect. Fig. 1 illustrates the main steps of the proposed methodology.

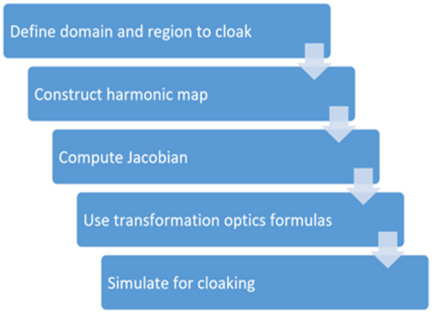


**Figure 1.** Flow chart of the proposed method

Cite as: N.A. Rehman, M. Raza, O. Rybin, S. Shulga, East Eur. J. Phys. 1, 484 (2026), https://doi.org/10.26565/2312-4334-2026-1-55

According to Fig. 1, the transformation domain and cloaked region are first defined. Using these, transformed coordinates are obtained through a harmonic map with appropriate boundary conditions. The corresponding Jacobian matrices are then computed at domain points, and the tensor field matrices are derived using transformation optics formulas. Finally, the cloaking configuration is simulated.

## METHODS AND RESULTS

The main target of this study is to design a transformation from virtual space to physical space providing the cloak invisibility for a circular region. The appropriate transformation $F$ is based on harmonic mapping.

The cloak phenomenon in a region is going to be confirmed in this study by absence or minimization of the energy of field coming to the region from outside. Accepting that the Laplace equation as a governing one in the study, one can estimate the above field energy by the energy functional $EN(F)$ given by

$$EN(F)=\frac{1}{2}\int_{\Omega}\|\nabla F\|^2 d^3\vec{r}\,, \tag{1}$$

where $\Omega$ is the virtual space.

### The Problem Statement

Consider three circles $C_i$ ($i=0,1,2$) with radius $r_i$ respectively with centers at the origin $(0,0)$ in 2-D Cartesian coordinate system $(x,y)$. Let $R_i$ be the region inside the circles $C_i$. Define the annular regions $\Omega=R_2\setminus R_0$ and $D=R_2\setminus R_1$, and construct a harmonic map $F:\Omega\to D$ defined as:

$$F(x,y)=(F_1(x,y),F_2(x,y))\,, \tag{2.1}$$

where $\forall(x,y)\in\Omega$ the following boundary conditions are imposed:

$$\left.\begin{aligned}&\forall(x,y)\in C_2:(F_1,F_2)\in C_2,\\&\forall(x,y)\in\left\{(x,y)\,|\,r_0^2\le x^2+y^2\le r_1^2\right\}:(F_1,F_2)\in C_1.\end{aligned}\right\} \tag{2.2}$$

For the sake of clarity, we assume in this study the that: $r_0=0.3$, $r_1=1$, $r_2=2$. It is assumed that a domain around of the origin is to be cloaked. In order to succeed, we are going to minimize the functional $EN(F)$ subject to constraints in the form of Eqs. (2), to further compute the desired transformation.

The setup of the study in the form of Eqs. (2a) is presented in Fig. 2 where the domain region depicted in the Figure part (a) is the virtual domain. Figure 2(b) shows the target region (the physical domain) which is to be achieved after applying the optimized (minimized) functional $EN(F)$.

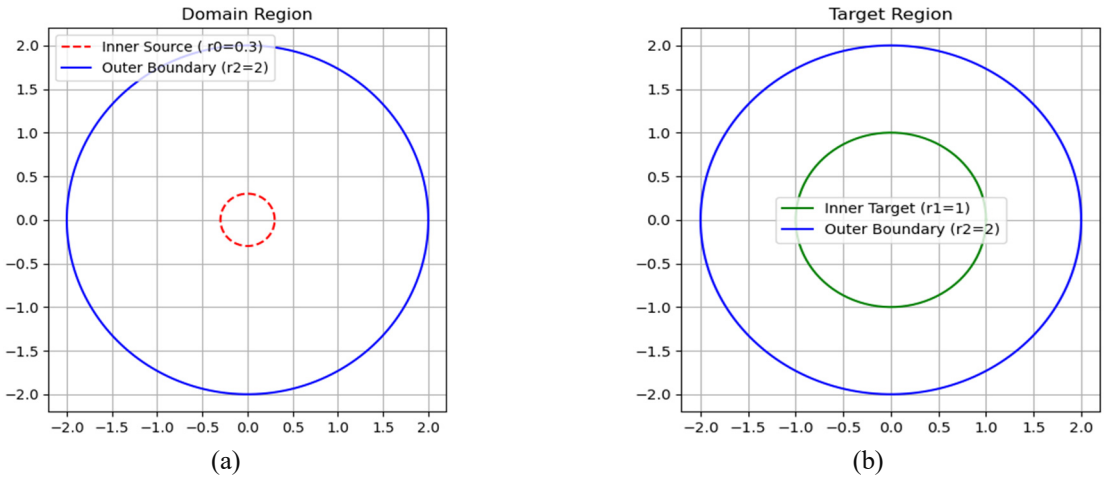


**Figure 2.** Setup of study for (a) virtual space, (b) physical space.

In the next section, as one of the targets of our study, we use neural network computations and get the transformation based on harmonicity of the functional $EN(F)$.

### PINNs Setup

To minimize energy functional (1) subject to constraints (2), we setup a neural network of four layers with two hidden layers, one input and one output layer. Input $(x,y)$ and output $F(x,y)=(F_1(x,y),F_2(x,y))$ layers have two

neurons. Each hidden layer has 32 neurons. We have used here the function $\sigma = \tanh(\cdot)$ as an activation function. Layers relations can be represented by the system:

$$\left.\begin{aligned} U_{n+1} &= \sigma(W_n U_n + b_n),\ n = 1,2, \\ U_1 &= (x,y)^T, \\ U_4 &= W_3 U_3 + b_3 = (F_1(x,y),\ F_2(x,y))^T. \end{aligned}\right\} \tag{3}$$

The output of the previous layer is the input of next layer. $W_1$ is weight matrix of order $32\times 2$, $W_2$ and $W_3$ are weight matrices of order $32\times 32$, $W_4$ is a weight matrix of order $2\times 32$. We take the weight matrix entries as random normal distribution to minimize loss as suggested for PINNs, [19-21]. Bias matrix $b_n$, $(n = 1,2,3)$ each of order $32\times 1$, $b_4$ is of order $2\times 1$, with constant entries 0. We take collocation points $N_\Omega = 1000$ in annular region $\Omega$, boundary points on $C_2$ as $N_2 = 200$, points on $\{(x,y) \mid 0.09 \le x^2 + y^2 \le 1\}$ as $N_0 = 300$.

Under the above assumptions, the mean square error or loss has been computed in this study by the formula:

$$\begin{aligned} MSE &= MSE_{\text{annular region }\Omega} + MSE_{\{0.3\le x^2+y^2\le 1\}} + MSE_{\text{boundary } C_2} \\ &= \frac{1}{N_1}\sum_{i=1}^{N_1}\left[\left(\frac{\partial^2 F_1}{\partial x^2}\right)_i + \left(\frac{\partial^2 F_1}{\partial y^2}\right)_i\right]^2 + \left[\left(\frac{\partial^2 F_2}{\partial x^2}\right)_i + \left(\frac{\partial^2 F_2}{\partial y^2}\right)_i\right]^2 + \frac{1}{N_0}\sum_{j=1}^{N_0}\left|norm\left(F_{\{0.3\le x^2+y^2\le 1\}}\right)_j - 1\right|^2 \\ &+ \frac{1}{N_2}\sum_{k=0}^{N_2}\left|\left(F_{\text{outer boundary}}\right)_k - (x,y)_k\right| = 0.02. \end{aligned} \tag{4}$$

The graph showing loss during training of our PINN for obtaining the optimal value of the $MSE$ is depicted in Fig. 3.

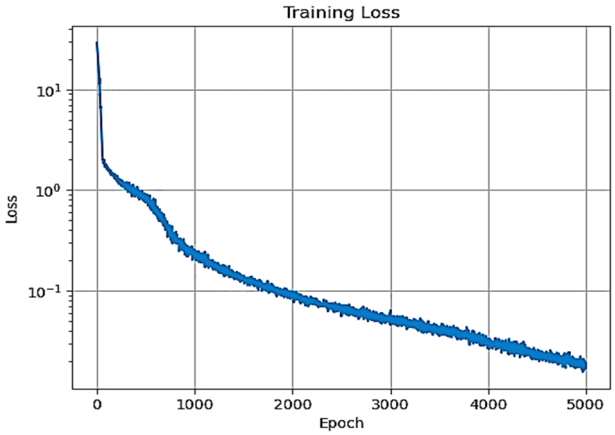


**Figure 3.** Graph of loss curve obtained during training PINN

The results of prediction of the map $F$ during training PINN are shown Figure 4: the graph (a) shows original grid in domain $\Omega$ while the graphs (b) stands for the already mapped (target) domain after applying the map $F$ to the grid depicted in graphs (a).

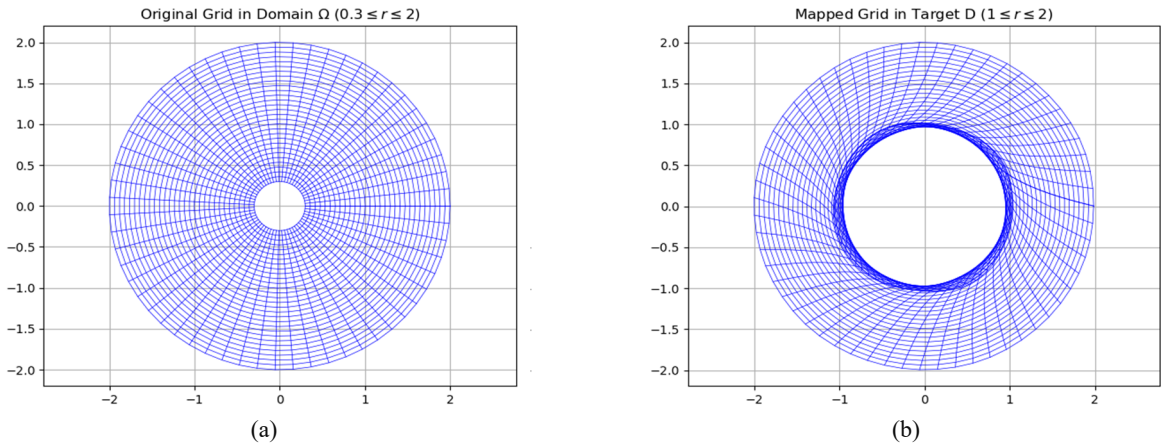


**Figure 4.** Transforming domain $\Omega$ by using the obtained optimized map $F$.

As a next step (as per the flow chart of Fig.1), we evaluate the Jacobean $J_F$ based on the predicted values of map $F(x,y)$:

$$J_F = \begin{bmatrix} \frac{\partial F_1}{\partial x} & \frac{\partial F_1}{\partial y} \\ \frac{\partial F_2}{\partial x} & \frac{\partial F_2}{\partial y} \end{bmatrix}, \tag{5}$$

where partial derivatives of $F(x,y)$ have been computed by calling *tf.gradient* function in tensor flow by above neural setup.

Then material tensor $A(x,y)$ given by

$$A = \frac{J_F J_F^T}{\det J_F}, \tag{6}$$

has been computed at all domain points.

We get symmetric positive definite material tensor $A(x,y)$ of order $2\times 2$, $\forall (x,y)\in \Omega$.

**Cloak Setup**

Throughout the study, the field distribution in the region $\Omega$ is defined by the two-dimensional potential $u(x,y)$. This means that the govern equation of the original region/domain is the isotropic Laplace equation:

$$\nabla^2 u = 0, \tag{7}$$

while the governing equation of the target region/domain is already the anisotropic Laplace equation:

$$\nabla(A\nabla u) = 0. \tag{8}$$

due to the tensor *A*.

Notice that physically material tensor *A* shows directional conductivity, the flux or flow vector which can be defined as $\vec{q} = -A\nabla u$.

Taking into account the definition of the harmonic map (2) leads to Dirichlet's problem for the potential $u(x,y)$ in the target domain:

$$\left.\begin{array}{l} \nabla(A\nabla u) = 0, \\ \begin{cases} u(x,y) = 0 & \forall (x,y)\in C_1 \\ u(x,y) = 1 & \forall (x,y)\in C_2 \end{cases}. \end{array}\right\} \tag{9}$$

where $C_1$ and $C_2$ are the inner and outer boundaries of already transformed region introduced in the Problem Statement section.

We solve Eqs. (9) using a neural setup. For this reason, we set up a five-layer neural network with three hidden layers, one input layer, and one output layer. Input $(x,y)$ and output $u(x,y)$ layers have two and one neurons respectively. Each hidden layer has 125 neurons. The activation function is $\sigma = \tanh(\cdot)$. The layers' relation mathematically is the same as explained in the PINNs Setup section. Thus, the mean square error/loss has been computed as:

$$MSE = MSE_{PDE} + MSE_{boundary\ C_2} = 0.2, \tag{10}$$

while Fig. 5 shows the plot of the solution.

One can see from the figure that Fig. 5(a) clearly reflects the Dirichlet boundary conditions, value of potential $u(x,y)$ is high at outer boundary and smoothly decreases up to inner boundary. At the same time, Fig. 5(b) shows the symmetry about an axis, say *z*-axis, reflecting the symmetry of material tensor. The surface curves are smoothly showing nonlinear variation of potential which is the result of anisotropic material tensor computed from transformation based on harmonicity of the mapping. Thus, both figures (a) and (b) show the effeteness of gradient distribution clearly showing a successful achieving the cloak phenomenon.

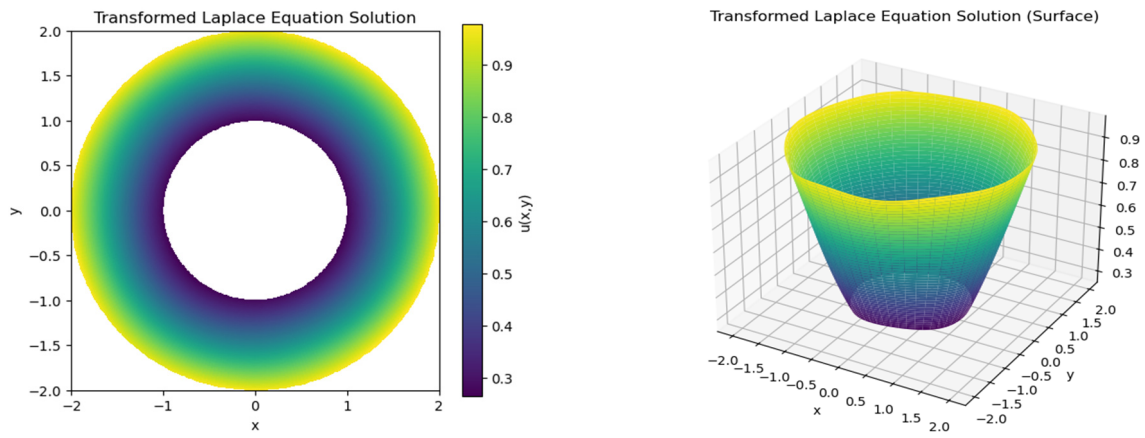


(a) (b)

**Figure 5. (a)** Clocked region and boundary. **(b)** Surface plot of anisotropic Laplace equation.

## DISCUSSION AND ANALYSIS

Further to show the effectiveness of proposed method based on harmonicity and neural computations, the gradient magnitude behaviour on transformed grid and radial profile have been plotted in Fig. 6. Smoothness and continuity show a weak distortion outside the cloaked region and there is smooth transition between cloaked and uncloaked region.

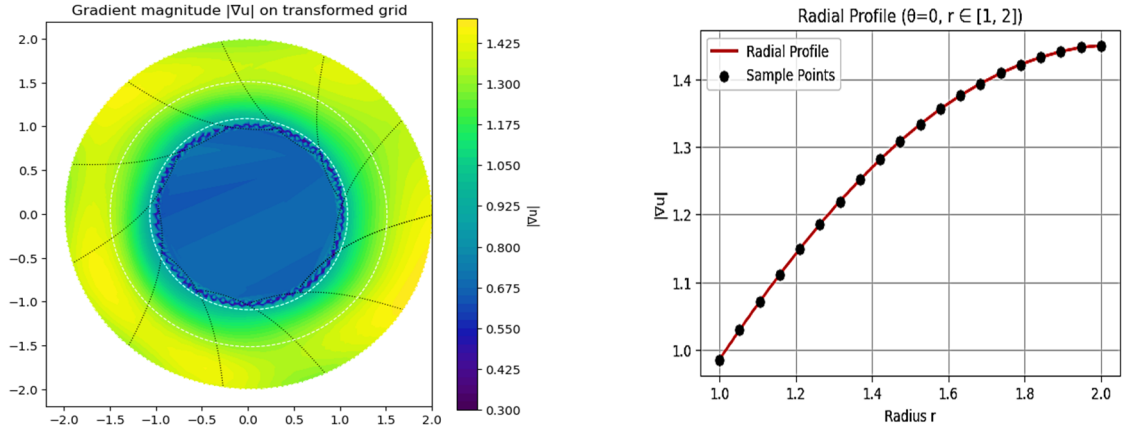


(a) (b)

**Figure 6. (a)** Gradient magnitude of potential on transformed grid. **(b)** Radial profile of Gradient magnitude of potential.

Resuming the results of previous section, one can clearly observe that Fig. 5-6 show how the transformation affects the gradient by compressing the potential variation near the inner region, making it appear as if the solution is smoothly pushed upward. This behaviour is consistent with cloaking mappings, where the anisotropic tensor redistributes the flow around the cloaked region without allowing penetration. It, in fact, enable to use the proposed method for masking the objects situated in the origin.

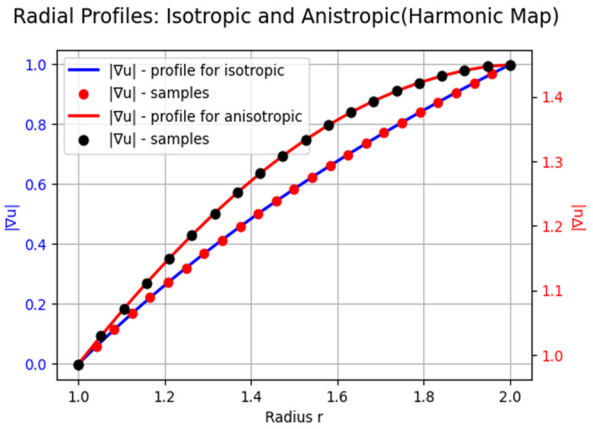


**Figure 7.** Radial Profile of gradient magnitude.

In Fig. 7, the radial profile of the magnitude of has been compared for isotropic and anisotropic cases (with harmonic transformation). In both cases, the radial profile increases with respect to radius *r,* however, in the anisotropic case, the gradient grows more rapidly. For the isotropic case, the magnitude of $\nabla u$ for origin domain increases approximately linearly with $r$ while in the anisotropic case (this is, in fact, rather relative to $A\nabla u$ ), the harmonic map based transformation modifies the radial scaling, resulting in an amplified gradient magnitude. Physically, this implies that the gradient exhibits stronger behavior near the outer boundary in the transformed medium which is important with a viewpoint of masking applications, in particular patch antenna masking.

## CONCLUSIONS

In this study, a new transformation model based on harmonic mapping has been created for designing 2-D circular cloaking structures. The model provides an alternative to conventional radial-based coordinate transformations widely used in applications of trans-formative optics. While computing the transformation coordinates under boundary constraints composed on the mapping, the resulting tensor field remains smooth. Numerical simulations of the transformed governing equation have confirmed that the proposed framework achieves effective field redirection with extremely weak scattering and distortion as well as stronger behaviour of the transformed field near the outer boundary. This new approach may be further adapted to diverse applications including object masking, in particular patch antennas.

The study shows the prospects for joint use harmonic mapping and methods of transformation optics as multidisciplinary subject.

### Acknowledgments

O. Rybin, and S. Shulga are grateful to the National Research Foundation of Ukraine for support of this work through the project grant (No. 2025.06/0108).

### ORCID

**Najma Abdul Rehman,** https://orcid.org/0000-0001-8952-8968; **Muhammad Raza**, https://orcid.org/0000-0002-1026-0856
**Oleg Rybin**, https://orcid.org/0000-0002-4472-6861; **Sergey Shulga,** https://orcid.org/0000-0002-9392-9366

### REFERENCES

[1] J. H. Samson, Annales scientifiques de l'É.N.S. 4e série. **11**(2), 211-228 (1978). https://doi.org/10.24033/asens.1344
[2] J. Eells, and L. Lemaire, Bull, London Math. Soc. **20**, 385-524. https://doi.org/10.1112/blms/10.1.1
[3] C.W. Misner, Physical Review D, **18**(12), 4510-4524 (1978). https://doi.org/10.1103/PhysRevD.18.4510
[4] X Zhai, C. Huang, & G. Ren, Scientific Reports, **10**, 18281 (2020). https://doi.org/10.1038/s41598-020-75211-5
[5] Q. Zhao, J. Liang, and Z. Xu, The Journal of Chemical Physics, **149**, 084111 (2018), https://doi.org/10.1063/1.5044438
[6] E. Chong, L. Zhang, and V.J. Santos, The International Journal of Robotics Research, **40**(2-3), 534-537 (2020). https://doi.org/10.1177/0278364920962205
[7] M. Kazemia, and Y.J. Moghaddam, Journal of Finsler Geometry and its Applications, **6**(1), 23-25 (2025). https://doi.org/10.22098/jfga.2024.16018.1140
[8] J.B. Pendry, *et al*. Science, **312**(5781), 1780-1782 (2006). https://doi.org/10.1126/SCIENCE.1125907
[9] L. Zhou, Brazilian Journal of Physics, **46**(1), 35-40 (2016). https://doi.org/10.1007/s13538-015-0378-z
[10] L. Zeng, and W. Xie, Modern Physics Letters B, **32**(21) 1850237 (2018). https://doi.org/10.1142/S0217984918502378
[11] J.B. Pendry, Y. Luo, & R. Zhao, Science, **348**(6234), 521-524 (2015). https://doi.org/10.1126/science.1261244
[12] H. Kan, L. Xu, Y. Xu, and H. Chen, Europhysics Letters, **117**(3), 34002 (2017). https://doi.org/10.1209/0295-5075/117/34002
[13] M.S. Khan, R.A. Shakoor, O. Fayyaz, and E.M. Ahmed, Optik, **297**, 171575 (2024). https://doi.org/10.1016/j.ijleo.2023.171575
[14] J.-H. Huang, H.-J. Ren, & T.-Y. Huang, Scientific Reports, **15**, 9427 (2025). https://doi.org/10.1038/s41598-025-94344-z
[15] M. Raza, Materials Research Express, **7**(5), 055802 (2020). https://doi.org/10.1088/2053-1591/ab8fba
[16] M. Raza, M. Ahsan, W.B. Alonazi, S.A. Naqvi, and B. Braaten, Physica Scripta, **98**(11), 115029 (2023). https://doi.org/10.1088/1402-4896/acfc6e
[17] J. Zhan, K. Li, Y. Zhou, X. Liu, and Y. Ma, ACS Applied Materials & Interfaces, **13**(14), 17104-17109 (2021). https://doi.org/10.1021/acsami.1c02117
[18] O. Rybin, M. Raza, S. Shulga, and N.A. Rehman, Zeitschrift für Naturforschung A, **80**(5), 335-344 (2025). https://doi.org/10.1515/zna-2024-0206
[19] M. Raissi, and G.E. Karniadakis, Journal of Computational Physics, **357**, 125–141 (2018). https://doi.org/10.1016/j.jcp.2017.11.039
[20] Z. Fang, and J. Zhan, IEEE Access, **8**, 24506–24513 (2019). https://doi.org/10.1109/ACCESS.2019.2963375
[21] A. Farea, O. Yli-Harja, and F. Emmert-Streib, Artificial Intellect, **5**(3), 1534-1557 (2024). https://doi.org/10.3390/ai5030074

## ВПРОВАДЖЕННЯ ГАРМОНІЧНОГО ЗОБРАЖЕННЯ ДЛЯ ФЕНОМЕНА НЕВИДИМОСТІ

**Найма Абдул Рехман[1], Мухаммед Раза[1], Олег Рибін[2], Сергій Шульга[2]**
*[1]Кафедра математики, Ісламабадський університет інформаційних технологій, Сагівальський кампус, Сагівал, Пакистан,*
*[2]Факультет радіофізики, біомедичної електроніки та комп'ютерних систем, Харківський національний університет імені В.Н. Каразіна, Харків, Україна*

У даній роботі для реалізації феномену маскування було застосовано новий підхід, заснований на фізичній трансформації. Вперше було отримано трансформаційне відображення шляхом мінімізації енергетичного функціоналу з урахуванням заданих геометричних обмежень, накладених на межі розсіювача. Ця варіаційна задача була вирішена шляхом застосування фізично-інформованої нейронної мережі для вирішення граничної задачі для рівняння Лапласа. Чисельний аналіз і графічна візуалізація отриманих результатів чітко демонструють слабке розсіювання і спотворення, а також незначне збурення зовнішніх полів. Крім того, ми показуємо, що запропоноване відображення дозволяє досягти значно кращих результатів у порівнянні з традиційними методами маскування на основі перетворення.

**Ключові слова:** *гармонічне відображення; фізично-інформованої нейронної мережі; невидимість; рівняння Лапласа; мінімізація енергетичного потенціалу*